Available online at www.sciencedirect.com

SciVerse ScienceDirect

Physics Procedia 27 (2012) 264 – 267

Physics Procedia

ISS2011

Relation of *n*-value to critical current in bent-damaged Bi2223 composite tape

S. Ochiai[a*], H. Okuda[a], M. Sugano[b], M. Hojo[a], K. Osamura[c], T. Kuroda[d], H. Kumakura[d], H. Kitaguchi[d], K. Itoh[d], H. Wada[d]

[a] *Graduate School of Engineering, Kyoto University, Yoshida, Sakyo-ku, Kyoto 606-8501, Japan.*
[b] *High Energy Accelerator Research Organization (KEK), Cryogenics Science Center, J-PARC Center, Tokai-Mura, Ibaraki 319-1106, Japan.*
[c] *Research Institute for Applied Sciences, Sakyo-ku, Kyoto 606-8202, Japan.*
[d] *National Institute for Materials Science, 1-2-1, Sengen, Tsukuba, Ibaraki 305-0047, Japan.*

Abstract

The relation of *n*-value to critical current of bent-damaged $(Bi,Pb)_2Sr_2Ca_2Cu_3O_{10+\delta}$ (Bi2223) composite tape was studied experimentally and analytically. The experimental results showed that, under bending strain, the *n*-value decreased rather slightly with decreasing critical current in comparison with the data obtained under applied tensile strain. The experimentally observed slight decrease in *n*-value with critical current under bending strain, and the measured changes in critical current and *n*-value with increasing bending strain, were described satisfactorily by the presented damage evolution model that correlates the extent of damage to variation of bending strain-induced tensile strain in the core along the thickness direction.

Keywords: Bi2223 composite tape; Critical current; *n*-value; Bending strain; Damage evolution

1. Introduction

Critical current of filamentary composite superconductor tapes under applied tensile/bending strain decreases beyond the irreversible strain due to crack evolution [1-7]. In the case of bending strain (ε_B) application, the damage extension is caused by the tensile strain in the sample length direction [2,3,7]. The tensile strain varies steeply along the thickness direction. Thus the outer side from the neutral axis is cracked severely, while the inner side near the neutral axis is less cracked. On the other hand, in the case of tensile strain (ε_T) application, the weaker filaments within the gauge length are predominantly cracked and then the stress concentration arising from the cracked filaments causes collective cracks (cracks composed of successively cracked filaments in a transverse cross-section), reducing critical current seriously [5]. Due to the difference in crack evolution behavior, it is expected that the relation of *n*-value to critical current under bending strain is different from that under tensile strain, as deduced from the relatively small reduction in *n*-value with increasing bending strain [4]. However, the relation of *n*-value to critical current under bending strain has not been studied in detail from the fracture mechanical viewpoint. The aim of the present work was to reveal the relation experimentally for $(Bi,Pb)_2Sr_2Ca_2Cu_3O_{10+\delta}$ (Bi2223) composite tape and to describe the experimental results by a damage evolution model.

* Corresponding author. Tel.: +81-75-753-4834 ; fax: +81-75-753-4841 .
E-mail address: shojiro.ochiai@materials.mbox.media.kyoto-u.ac.jp .

1875-3892 doi:10.1016/j.phpro.2012.03.461

2. Experimental procedure

The VAM1 sample supplied during a round robin test [4] of VAMAS/TWA 16 was used for experiment. Bending strain ε_B was given at room temperature by pressing the specimens with the upper GFRP (Glass Fiber Reinforced Plastic) die to the lower one with the same curvature [4]. The specimens bent at room temperature were cooled down to 77 K, at which E(electric field) –I(current) curves were measured with a usual four probe-method in a self magnetic field for a voltage probe-distance 2 cm. The critical current (I_c) values were estimated with a criterion of E_c=1 μV/cm. The n-value was estimated by fitting the measured E-I curve with $E=E_c(I/I_c)^n$ for the electric field range of E=0.2 μV/cm–10 μV/cm. The I_c - and n-values at ε_B = 0, 0.2, 0.4, 0.6, 0.8 and 1.0 % were estimated for three samples (S1, S2 and S3).

3. Results and discussion

3.1. Experimental results

The changes in measured I_c- and n-values with ε_B are shown in Fig. 1(a, b). The correlation of n- to I_c- value is shown in (c). In addition to the experimental results, the averages of I_c and n-value measured in the round robin test, reported in Ref. [4], are shown with ∇ for reference.

The n–I_c relation under tensile strain was also measured for two samples. The n–I_c relations under both strains are shown in Fig. 2. The decrease in n-value with I_c under bending strain was rather slight in comparison with that under tension. We attempted to account for and to reproduce the measured slight decrease under bending strain by modeling analysis, whose procedure is shown below. The result of the modeling analysis is superimposed in Fig. 1, describing the experimental results satisfactorily.

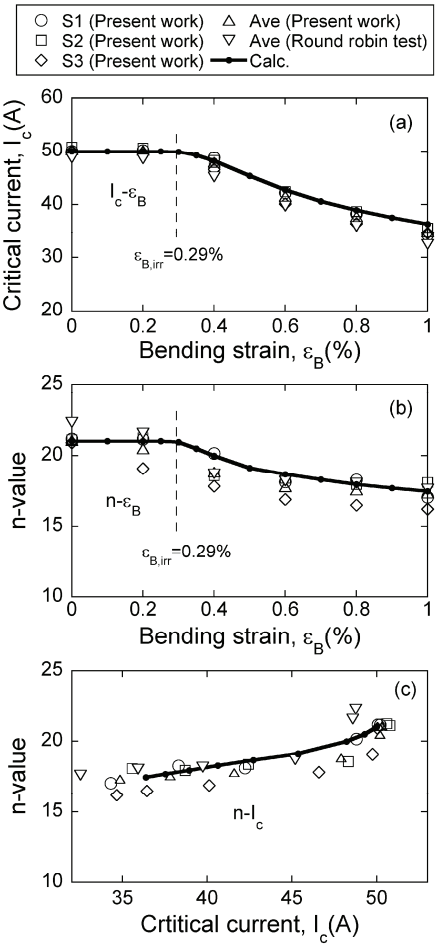

Fig. 1. Results of experiment and modeling analysis. (a) and (b) show the change in I_c- and n-values with increasing ε_B. The measured values of the samples S1, S2 and S3 are shown with ○, □ and ◊, respectively. The averages of I_c- and n-values of them at each ε_B tested are shown with Δ. The averages of I_c- and n-values measured in the round robin test [4] are shown with ∇ for reference. (c) shows the n-I_c relation. The results of modeling analysis are shown with solid curves.

3.2. Formulation of damage evolution under bending strain

The present sample was composed of the core in which the filaments are bundled into Ag and the sheath of Ag alloy. Figure 3(a) shows a micrograph of the transverse cross-section of the sample, in which the thickness direction is three times magnified from the as-observed one as to show clearly the shape of the core. The core boundary is shown with the broken curve. Figure 3(b) shows the schematic representation of the transverse cross-section, in which W_{core} (=3.52 mm) and t (=0.270 mm) are the width of the core and thickness of the sample, respectively, and x and y refer to the distances from the center of the composite tape (x=y=0) in the width and thickness directions, respectively. The core boundary y_{core} (ABCD) can be expressed as a function of x [2].

The maximum value of y_{core}, $y_{core,max}$, corresponding to the location of the core nearest to the outer surface of the sample, was 0.117 mm. Under application of bending strain, the damage of Bi2223 filaments takes place first at y=$y_{core,max}$ when ε_B reaches $\varepsilon_{B,irr}$. Beyond $\varepsilon_{B,irr}$, the damage front extends towards y=0 (neutral axis) with increasing ε_B, causing further reduction in critical current.

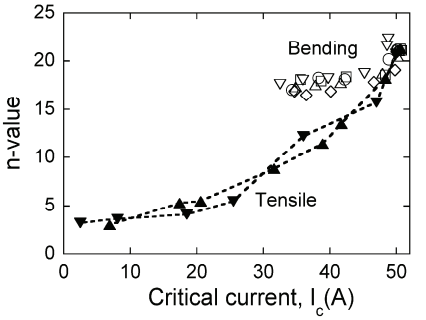

Fig. 2. Comparison of the n-I_c relation under bending strain with that under tensile strain.

Under bending strain, cracking of filaments is caused by the tensile strain in the longitudinal direction [2,3]. The tensile strain varies steeply along the thickness direction. Accordingly, the extent of damage is dependent on location in the core. To describe the change in I_c and n-value with increasing ε_B, the relation of bending strain-induced tensile strain to the location-dependent extent of damage is needed.

Under tensile strain ε_T, cracking of the filaments occurs first at the irreversible tensile strain $\varepsilon_{T,irr}$. In the later stage, all filaments are cracked in a cross-section. Such a tensile strain is noted as $\varepsilon_{T,m}$. When tensile strain is raised further, multiple cracking of filaments (once-cracked filaments in a cross-section are further cracked continually in other cross-sections) takes place. Due to the specific features of the tensile stress-strain curve in $\varepsilon_T<\varepsilon_{T,irr}$, $\varepsilon_{T,irr}<\varepsilon_T<\varepsilon_{T,m}$ and $\varepsilon_{T,m}<\varepsilon_T$ shown below, the $\varepsilon_{T,irr}$- and $\varepsilon_{T,m}$- values can roughly be estimated from the stress-strain curve [7], as follows.

Figure 4(a) shows the measured tensile stress (σ_T)–strain (ε_T) curve of the sample at room temperature. The sample deforms at nearly constant stress at high strain range (ε_T>0.3 %), where the loss of stress-bearing capacity due to multiple cracking of filaments is balanced with the strain hardening-induced increase in stress carrying capacity of the Ag and Ag alloy [3,5,7]. The filament cracking initiates in advance of such a stress-constant stage [2,5,7]. The stress-strain range, covering the cracking- initiation and -evolution stage and part of multiple cracking stage, is shown with a rectangle in Fig. 4(a). In the former stage, filaments-cracking causes reduction in slope of the stress-strain curve. In the latter stage, the slope becomes zero. The variation of the slope $d\sigma_T/d\varepsilon_T$ with strain ε_T is shown in Fig. 4(b). The $\varepsilon_{T,irr}$ was estimated to be 0.25 % from the tensile strain ε_T at initiation of the reduction in slope. The $\varepsilon_{T,m}$ was estimated to be 0.32 % from ε_T at which the slope reaches zero.

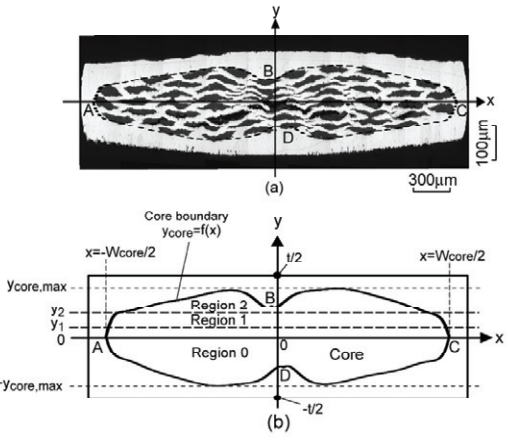

Fig. 3. (a) Micrographs of the transverse cross-section of the sample, in which the thickness direction is three times magnified from the as-observed one, and (b) the schematic representation of the shape of the core in the transverse cross-section and damage front y_1 and y_2. Regions 0, 1 and 2 refer to the non-damaged, partially damaged and seriously damaged regions in the core, for $-y_{core,max}<y<y_1$, $y_1<y<y_2$ and $y_2<y<y_{core,max}$, respectively.

Using the results above, three regions are characterized; Region 0 (non-damaged region) for $\varepsilon_T<\varepsilon_{T,irr}$ where all filaments transport current and critical current is retained, Region 1 (partly damaged region) for $\varepsilon_{T,irr}<\varepsilon_T<\varepsilon_{T,m}$ where cracked and non-cracked filaments co-exist and hence critical current is reduced but not to zero, and Region 2 (seriously damaged region) for $\varepsilon_T>\varepsilon_{T,m}$ where all filaments are cracked and critical current is very low. Under bending strain, Regions 0, 1 and 2 also appear, as schematically shown in Fig. 3(b), since the tensile strain varies steeply along the thickness direction. Noting the damage fronts corresponding to $\varepsilon_{T,irr}$ and $\varepsilon_{T,m}$ as y_1 and y_2, respectively, Regions 0, 1 and 2 exist in $-y_{core,max}<y<y_1$, $y_1<y<y_2$ and $y_2<y<y_{core,max}$, respectively. The relation of y_1 to $\varepsilon_{T,irr}$ and that of y_2 to $\varepsilon_{T,m}$ at ε_B are expressed as [2,7]

$$y_1=\varepsilon_{T,irr}/\{\varepsilon_B/(t/2)\},\quad y_2=\varepsilon_{T,m}/\{\varepsilon_B/(t/2)\} \qquad (1)$$

where t is the thickness of the sample (0.27 mm). Substituting $\varepsilon_{T,irr}$=0.25 % and $\varepsilon_{T,m}$ =0.32 % and t=0.27 mm into Eq.(1), we have y_1 and y_2 as a function of ε_B. Here we define the cross-sectional area of the core as S_{core}(=0.646 mm^2) and the cross-sectional areas of Regions 0, 1 and 2 as ΔS_0, ΔS_1 and ΔS_2, respectively. By calculation of the cross-sectional area with the core boundary y_{core}, and location of y_1 and y_2, we have $\Delta S_0/S_{core}$, $\Delta S_1/S_{core}$ and $\Delta S_2/S_{core}$ also as a function of ε_B, as shown in Fig. 5. For $\varepsilon_B\le\varepsilon_{B,irr}$ where filaments were not cracked, $\Delta S_0/S_{core}$ remained 1(unity). When ε_B reached $\varepsilon_{B,irr}$ (0.29 %, which was obtained by substituting $y_1=y_{core,max}$(=0.117 mm), t=0.27 mm and $\varepsilon_{T,irr}$=0.25 % into Eq.(1)), Region 1 appeared. Region 2 appeared at ε_B=0.37 %, which was obtained by substituting

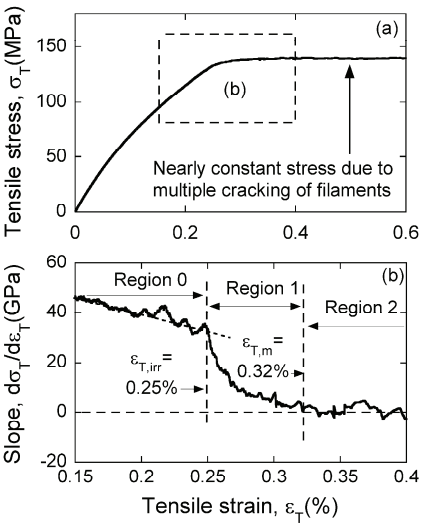

Fig. 4. (a) Measured tensile stress (σ_T) –strain (ε_T) curve of the sample at room temperature. The arrow shows the stage of multiple cracking of Bi2223 filaments. The slope of the region surrounded by the rectangle in (a), where cracking initiates and evolutes, is presented in (b). The estimated values of $\varepsilon_{T,irr}$ and $\varepsilon_{T,m}$, and Regions 0, 1 and 2 are indicated in (b).

$y_2=y_{core,max}$, t and $\varepsilon_{T,irr}$=0.32 % into Eq. (1). The $\Delta S_1/S_{core}$ was less than 0.08 in $\varepsilon_{B,irr}<\varepsilon_B<1.0$ %. The $\Delta S_2/S_{core}$ increased largely with ε_B, reaching around 0.26 at ε_B=1.0 %.

3.3 Estimation of critical current and n-value

Regarding the sample to be composed of a parallel circuit of Regions 0, 1 and 2, we can calculate E - I curve by

$$I = \sum_{i=0}^{2} I_{c,i}(\Delta S_i / S_{core})(E / E_c)^{1/n_i} \quad (2)$$

where $I_{c,i}$ and n_i are the I_c- and n-values of Region i (i = 0, 1 and 2), respectively. For Region 0, $I_{c,0}$ and n_0 were taken to be 50 A and 21 from the average critical current and n-value measured at ε_B=0 %, respectively. For Region 1, a half of the $I_{c,0}$ was taken as $I_{c,1}$ (25 A). The corresponding n-value, n_1, was taken to be 6 from the experimental results under tensile strain (Fig. 2). For Region 2, $I_{c,2}$ and n_2 were taken to be 2.5 A and 3.2, respectively, from the lowest set of I_c and n-value measured under tensile strain shown in Fig.2. Substituting the values of $I_{c,i}$ and n_i stated above and the values of $\Delta S_i/S_{core}$ (Fig. 5) into Eq.(2), E–I curve was calculated, from which I_c (1 μV/cm criterion) and n-value (E=0.2~10 μV/cm) were estimated at each ε_B. The calculated changes in I_c- and n-values with increasing ε_B and correlation of n-value to I_c are superimposed in Fig.1. The experimental results are described satisfactorily.

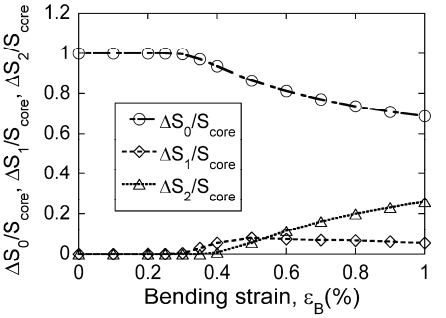

Fig. 5. Change in fraction of cross-sectional area of Region 0 ($\Delta S_0/S_{core}$), Region 1 ($\Delta S_1/S_{core}$) and Region 2 ($\Delta S_2/S_{core}$) with increasing bending strain ε_B.

The calculated critical current at ε_B=0.6 % for instance was 42.1 A. The calculated currents transported by Regions 0, 1 and 2 were 40.6, 1.8 and 0.3 A, respectively. Current was mostly transported by Region 0. For other bending strains, the situation was the same. In the whole range of ε_B investigated, at and in the neighborhood of E=E_c, more than 95 % of the current was transported by Region 0. This result means that, while the currents transported by Regions 1 and 2 are low, the lower n-values of Regions 1 and 2 still act to reduce slightly the n-value of the sample.

4. Conclusions

(1) Changes in critical current and n-value of Bi2223 composite tape with increasing bending strain were measured, from which the relation of n-value to critical current was obtained and was compared with the data obtained under tensile strain. It was shown that, under bending strain, the n-value decreased rather slightly with decreasing critical current, while, under tensile strain, it decreased significantly.

(2) A damage evolution model was presented to describe the experimental results. In the modeling, the correlation among the steep variation of tensile strain along the thickness direction under bending strain, shape of the core and extent of damage in the core was formulated.

(3) With the presented model and procedure for calculation, the measured relation of n-value to critical current under bending strain, featured with a slight decrease in n-value with decreasing critical current, and the measured changes in critical current and n-value with increasing bending strain, were described satisfactorily.

Acknowledgement

The authors wish to express their gratitude to The Ministry of Education, Culture, Sports, Science, and Technology, Japan for the grant-in-aid (no. 22360281).

References

[1] Kitaguchi H, Itoh K, Kumakura H, Takeuchi T, Togano K, Wada H. *IEEE Trans. Appl. Supercond*. 2001;11:3058-61.
[2] Ochiai S, Matsuoka T, Shin JK, Okuda H, Sugano M, Hojo M, Osamura K. *Supercond. Sci. Technol.* 2007;20:1076-83.
[3] Ochiai S, Shin JK, Iwamoto S, Okuda H, Oh SS, Ha DW, Sato M. *J. Appl. Phys.* 2008;103:123911.
[4] Kuroda T, Itoh K, Katagiri K, Goldacker W, Hsessler W, ten Haken B, Kiuchi M, Noto N, Ochiai S, Otabe S, Shin HS, Sosnowski J, Weijers H, Wada H, Kumakura K. *Physica C* 2005;425:111-20.
[5] Ochiai S, Nagai T, Okuda H, Oh SS, Hojo M, Tanaka M, Sugano M, Osamura K. *Supercond. Sci. Technol.* 2003;16: 988-94.
[6] Shin HS, Katagiri K. *Supercond. Sci. Technol.* 2003;16:1012-8.
[7] Ochiai S, Okuda H, Sugano M, Hojo M, Osamura K. *J. Appl. Phys.* 2010;107:083904.